6
Applications in deep inelastic scattering

The preceding chapters have established the theoretical framework which ought to describe the perturbative scattering of strongly interacting particles at high centre-of-mass energies (in the Regge region). In this chapter (and the next), we shall attempt to place this framework under the experimental spotlight. That is to say, we shall turn the theoretical calculations of the preceding chapters into physical cross-sections for processes which can be measured at present or future colliders.

To construct these cross-sections, we need to specify the impact factors which define the coupling of the Pomeron to the external particles. These impact factors are then convoluted with the universal BFKL amplitude, $f(\omega, \mathbf{k_1}, \mathbf{k_2}, \mathbf{q})$ (see Eq.(4.33)) in order to obtain the relevant elastic-scattering amplitude. Remember that we are using perturbation theory and so can take our result seriously only if we are sure that the typical transverse momenta are much larger than Λ_{QCD}. As we showed in Section 5.1, for $t = 0$ the largeness of the typical transverse momenta is assured provided we pick processes with impact factors which are peaked at large transverse momenta. Clearly, this is not the case for proton–proton scattering and that is why we were not surprised to find that our results were incompatible with the relatively modest rise of the p–p total cross-section with increasing s. Another way of keeping our integrals away from the infra-red region is to work at high-t but we defer this topic until the next chapter.

In this chapter we shall focus on the process of deep inelastic lepton–nucleon scattering. In the centre-of-mass frame, the incoming lepton is scattered through a large angle, radiating a highly virtual photon (γ^*) which scatters inelastically off the incoming nucleon (let us say it is a proton, p). The total cross-section for $\gamma^* p \to X$ (where X labels all possible final states) is obtained by

https://doi.org/10.1017/9781009290111.008 Published online by Cambridge University Press

taking the imaginary part of the elastic $\gamma^* p \to \gamma^* p$ cross-section at $t = 0$ (recall the optical theorem of Chapter 1). For high γ^*–p centre-of-mass energies we can try to use the BFKL amplitude to compute this cross-section. As we shall see, the high virtuality of the γ^* provides the large scale in the associated impact factor. Unfortunately, we also need the impact factor associated with the proton line. In this case (as is also the case in p–p scattering) we have no large scale (indeed we cannot calculate this impact factor using perturbation theory) and as such must consider the fact that our transverse momentum integrals pick up significant contributions from the infra-red region.

After illuminating the above remarks, we will consider a process which should provide a much more direct test of the purely perturbative dynamics. By picking the impact factor associated with the proton such that it describes the production of a parton of high p_T into the final state, we can sidestep the infra-red problems which plague the deep inelastic total cross-section.

In Section 6.4, we shall discuss how our approach relates to the more conventional ('Altarelli–Parisi') one. To finish the chapter we demonstrate that the assumption of multi-Regge kinematics (i.e. strong ordering of the Sudakov components) is not in general suitable as we move away from the discussion of elastic-scattering amplitudes (and hence total cross-sections).

6.1 Introduction

The basic deep inelastic amplitude for electron–proton (e–p) scattering is shown in Fig. 6.1. The incoming electron and proton four-momenta are k and p, respectively, and the virtual (space-like) photon has four-momentum q. The important kinematic invariants are

$$\begin{aligned} Q^2 &= -q^2 > 0, \\ s &= (p+k)^2, \\ W^2 &= (p+q)^2, \\ x &= \frac{Q^2}{2p\cdot q} \approx \frac{Q^2}{Q^2+W^2}, \end{aligned}$$

https://doi.org/10.1017/9781009290111.008 Published online by Cambridge University Press

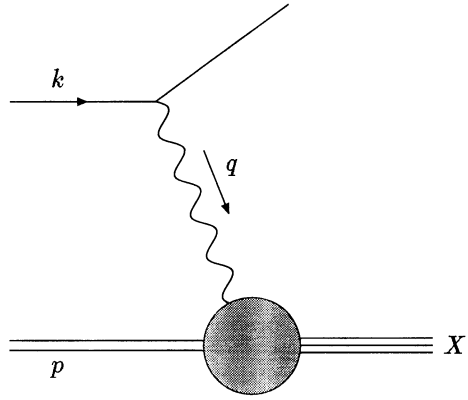

Fig. 6.1. The basic deep inelastic scattering process.

and

$$y = \frac{p \cdot q}{p \cdot k} \approx \frac{Q^2}{xs}.$$

The approximate equalities become exact in the limit of negligible lepton and proton masses. We shall subsequently assume this limit. As always, we also work in the high energy limit, i.e.

$$W^2 \gg Q^2 \gg M_p^2.$$

Since this inequality implies that $x \ll 1$ we say we are working in the low-x regime.

The total e–p cross-section can be written as a contraction of a lepton tensor (calculated purely within QED) and a hadronic tensor.† The hadronic tensor is then written in terms of two independent structure functions (utilizing gauge, Lorentz and time-reversal invariance, parity conservation and assuming unpolarized beams), i.e.

$$\frac{d^2\sigma}{dx dQ^2} = \frac{2\pi\alpha^2}{xQ^4}\left\{[1 + (1-y)^2]F_2(x,Q^2) - y^2 F_L(x,Q^2)\right\}, \quad (6.1)$$

where α is the fine structure constant. Given the assumptions, this is a completely general expression and tells us nothing about the

† For those readers unfamiliar with these details, we refer to the standard texts, e.g. Close (1979).

https://doi.org/10.1017/9781009290111.008 Published online by Cambridge University Press

functional form of structure functions. However, we can re-write them in terms of the cross-sections for scattering transverse or longitudinal photons off the proton, i.e.

$$\begin{aligned} F_2(x,Q^2) &= \frac{Q^2}{4\pi^2\alpha}(\sigma_T(x,Q^2)+\sigma_L(x,Q^2)) \\ F_L(x,Q^2) &= \frac{Q^2}{4\pi^2\alpha}\sigma_L(x,Q^2). \end{aligned} \tag{6.2}$$

Our goal in the next section will be to calculate these structure functions as far as is possible (we will struggle with the proton impact factor).

6.2 The low-x structure functions

We shall obtain the structure functions by computing the imaginary part of the amplitude for elastic $\gamma^* p$ scattering (for each photon polarization). In the high energy limit, for photons with polarization λ, we have (from Eq.(4.36))

$$\sigma_\lambda(x,Q^2) = \frac{\mathcal{G}}{(2\pi)^4}\int \frac{d^2\mathbf{k_1}}{\mathbf{k_1^2}}\frac{d^2\mathbf{k_2}}{\mathbf{k_2^2}}\Phi_\lambda(\mathbf{k_1})\Phi_p(\mathbf{k_2})F(x,\mathbf{k_1},\mathbf{k_2}), \tag{6.3}$$

where Φ_p is the proton impact factor and Φ_λ is the impact factor for a photon of polarization λ. This equation is shown graphically in Fig. 6.2 for one particular contribution to the photon impact factor (e.g. there are also contributions where the gluons couple to the different quark lines). Notice that we have shifted to a more convenient notation (with respect to Eq.(4.36)): we have suppressed all dependence on the momentum transfer $\mathbf{q}$ since it is zero and we have taken the inverse Mellin transform of the BFKL amplitude so as to obtain it as a function of $x \approx Q^2/W^2$.

We have already computed the BFKL amplitude (see Eq.(4.28)), i.e.

$$\begin{aligned} F(x,\mathbf{k_1},\mathbf{k_2}) &= \sum_{n=0}^{\infty}\int_{-\infty}^{\infty} d\nu \left(\frac{\mathbf{k_1^2}}{\mathbf{k_2^2}}\right)^{i\nu}\frac{e^{in(\theta_1-\theta_2)}}{2\pi^2 k_1 k_2} \\ &\quad\times \exp\left(\bar{\alpha}_s\chi_n(\nu)\ln 1/x\right). \end{aligned} \tag{6.4}$$

This is where the x-dependence of our final result resides and we can clearly see that the leading eigenvalue of the kernel leads to a

https://doi.org/10.1017/9781009290111.008 Published online by Cambridge University Press

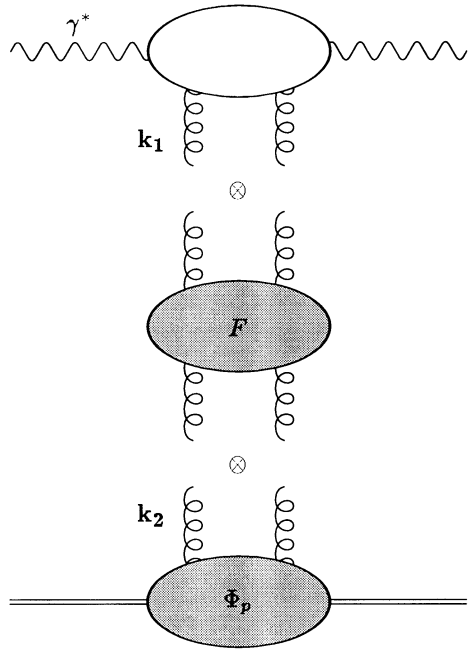

Fig. 6.2. One of the graphs contributing to the amplitude for elastic $\gamma^* p$ scattering. The '$\otimes$' symbols represent the convolution of the BFKL amplitude with the impact factors.

strong rise with decreasing x, i.e.

$$F \sim \frac{x^{-\omega_0}}{\sqrt{\ln 1/x}},$$

where ω_0 is as in Eq.(4.31), i.e. $\omega_0 = 4\bar{\alpha}_s \ln 2$.† This translates directly into the same rise at low x for the total deep inelastic scattering cross-section (i.e. the structure functions $F_2(x, Q^2)$ and $F_L(x, Q^2)$). We will discuss this behaviour and compare it with experimental data shortly. For now let us merely say that the data on low-x structure functions does indeed exhibit a strong rise with decreasing x. This is the first time a total cross-section has been measured which rises strongly with increasing centre-of-mass energy. Such a rise cannot be explained by the soft Pomeron

† Recall that $\bar{\alpha}_s = 3\alpha_s/\pi$ for the three colours of QCD.

https://doi.org/10.1017/9781009290111.008 Published online by Cambridge University Press

pole which describes so well the total hadronic cross-sections and we are therefore encouraged in our attempt to use perturbative QCD.

It only remains to compute the impact factors and perform the convolution. We are unable to compute the proton impact factor using perturbation theory and so we choose to take it as a phenomenological input. We expect it to describe some primordial gluon distribution in transverse momenta which is peaked around $\sim M_p$. The photon impact factor is calculable in perturbation theory. The calculation is detailed in Appendix A to this chapter.

Using these impact factors along with Eqs.(6.3) and (6.4), we can deduce the proton structure functions up to the largely unknown proton impact factor, $\Phi_p(\mathbf{k_2})$. Before discussing this procedure further we want to deviate a little in order to introduce the concept of the gluon distribution (or density) function.

We define the **unintegrated gluon density**, $\mathcal{F}(x,\mathbf{k})$, to be that (dimensionless) 'cross-section' which would be observed if the photon impact factor (Φ_λ) were replaced by the impact factor Φ_g where

$$\Phi_g(\mathbf{k_1}) = 2\pi\mathbf{k}^4\delta^2(\mathbf{k_1}-\mathbf{k}).$$

Thus we have the definition

$$\mathcal{F}(x,\mathbf{k}) \equiv \frac{1}{(2\pi)^3}\int \frac{d^2\mathbf{k}'}{\mathbf{k}'^2}\Phi_p(\mathbf{k}')\mathbf{k}^2 F(x,\mathbf{k},\mathbf{k}'). \tag{6.5}$$

The **gluon density** is then defined to be

$$G(x,Q^2) \equiv \int \frac{d^2\mathbf{k}}{\pi\mathbf{k}^2}\Theta(Q^2-\mathbf{k}^2)\mathcal{F}(x,\mathbf{k}), \tag{6.6}$$

where we have introduced the theta (step) function, $\Theta(Q^2-\mathbf{k}^2)$, which is defined to equal unity when $Q^2 > \mathbf{k}^2$ and zero when $Q^2 < \mathbf{k}^2$. This definition of the gluon density will be particularly useful when we come to make our comparisons with the Altarelli–Parisi approach to the structure functions at low x. For now it merely simplifies our notation. Note that $\mathcal{F}(x,\mathbf{k})$ contains the BFKL dynamics (convoluted with the proton impact factor) but that, unlike the structure functions, it is not a physical observable.

https://doi.org/10.1017/9781009290111.008 Published online by Cambridge University Press

The structure functions are thus given by

$$\begin{aligned} F_2(x,Q^2) &= \frac{Q^2}{4\pi^2\alpha}\int\frac{d^2\mathbf{k}}{\mathbf{k}^4}\frac{\mathcal{F}(x,\mathbf{k})}{4\pi}(\Phi_T(\mathbf{k})+\Phi_L(\mathbf{k})) \\ &= \frac{Q^2}{4\pi^2}\alpha_s\sum_{q=1}^{n_f}e_q^2\int\frac{d^2\mathbf{k}}{\mathbf{k}^2}\mathcal{F}(x,\mathbf{k})\int_0^1 d\rho d\tau \\ &\times\frac{1-2\rho(1-\rho)-2\tau(1-\tau)+12\rho(1-\rho)\tau(1-\tau)}{Q^2\rho(1-\rho)+\mathbf{k}^2\tau(1-\tau)} \end{aligned} \tag{6.7}$$

and

$$\begin{aligned} F_L(x,Q^2) &= \frac{Q^2}{4\pi^2\alpha}\int\frac{d^2\mathbf{k}}{\mathbf{k}^4}\frac{\mathcal{F}(x,\mathbf{k})}{4\pi}\Phi_L(\mathbf{k}) \\ &= \frac{2Q^2}{\pi^2}\alpha_s\sum_{q=1}^{n_f}e_q^2\int\frac{d^2\mathbf{k}}{\mathbf{k}^2}\mathcal{F}(x,\mathbf{k})\int_0^1 d\rho d\tau \\ &\times\frac{\rho(1-\rho)\tau(1-\tau)}{Q^2\rho(1-\rho)+\mathbf{k}^2\tau(1-\tau)}. \end{aligned} \tag{6.8}$$

We have multiplied by the factor $T(F)=\frac{1}{2}$, to account for the colour factor associated with the upper quark loop. The impact factors, Φ_T and Φ_L, are for scattering off transverse and longitudinal photons, respectively, and their calculation is detailed in Appendix A to this chapter.

Note that our definition of $G(x,Q^2)$ is such that, in the limit

$$\mathbf{k}^2 \ll Q^2$$

(which is equivalent to taking the leading log Q^2 approximation to the BFKL equation and is usually referred to as the **double leading log approximation**), we can write

$$\begin{aligned} \frac{\partial F_2(x,Q^2)}{\partial\ln Q^2} &= 2\sum_{q=1}^{n_f}e_q^2\frac{\bar{\alpha}_s}{6}\int_0^1 d\tau P_{qg}(\tau)G(x,Q^2) \\ &= \sum_{q=1}^{n_f}e_q^2\frac{\bar{\alpha}_s}{9}G(x,Q^2), \end{aligned} \tag{6.9}$$

where $P_{qg}(\tau)=\frac{1}{2}(\tau^2+(1-\tau)^2)$ is the usual Altarelli–Parisi splitting function. The key to obtaining this expression is to notice that, after differentiating Eq.(6.7) with respect to $\ln Q^2$, the dominant contribution to the ρ integral is from the end-points where ρ is within $\tau(1-\tau)\mathbf{k}^2/Q^2$ of either 0 or 1 (modulo terms which are

https://doi.org/10.1017/9781009290111.008 Published online by Cambridge University Press

suppressed by $\sim \mathbf{k}^2/Q^2$). Later we shall discuss the connection between the Altarelli–Parisi and the BFKL approaches in more detail.

Let us conclude this section by introducing a toy model for the proton impact factor. We can then compute the low-x structure functions. We will try an impact factor of the form

$$\Phi_p(\mathbf{k}) \sim \left(\frac{\mathbf{k}^2}{\mathbf{k}^2+\mu^2}\right)^{\delta}, \tag{6.10}$$

where μ is a scale which is typical of the non-perturbative dynamics and δ is essentially unknown (except that we know that $\delta > \frac{1}{2}$ in order that the $\mathbf{k}'$ integral is finite). The $\mathbf{k}'$ integral can now be performed since

$$\begin{aligned}\int \frac{d^2\mathbf{k}'}{\mathbf{k}'^2}\left(\frac{\mathbf{k}'^2}{\mathbf{k}'^2+\mu^2}\right)^{\delta}(\mathbf{k}'^2)^{-1/2-i\nu} \\ = \pi(\mu^2)^{-1/2-i\nu}\frac{\Gamma(\delta-1/2-i\nu)\Gamma(1/2+i\nu)}{\Gamma(\delta)}.\end{aligned} \tag{6.11}$$

Thus, in the $n=0$ limit, which selects the leading eigenvalue of the kernel (the angular integrals are then trivial), we have

$$\begin{aligned}\frac{\mathcal{F}(x,\mathbf{k})}{\mathbf{k}^2} &= \frac{\mathcal{N}_g}{2\pi}\int_{-\infty}^{\infty}\frac{d\nu}{\sqrt{\mu^2\mathbf{k}^2}}\left(\frac{\mathbf{k}^2}{\mu^2}\right)^{i\nu}\exp\left(\bar{\alpha}_s\chi_0(\nu)\ln 1/x\right) \\ &\quad\times\frac{\Gamma(\delta-1/2-i\nu)\Gamma(1/2+i\nu)}{\Gamma(\delta)}.\end{aligned} \tag{6.12}$$

The constant $\mathcal{N}_g$ contains the unknown normalization of the proton impact factor as well as the colour factor and factors of π. Substituting this into the expression for $F_2(x,Q^2)$, we can also perform the $\mathbf{k}$ integral, using

$$\begin{aligned}\int_0^{\infty}\frac{(\mathbf{k}^2)^{-1/2+i\nu}d\mathbf{k}^2}{Q^2\rho(1-\rho)+\mathbf{k}^2\tau(1-\tau)} &= \frac{\pi[\tau(1-\tau)]^{-1}}{\cosh\pi\nu} \\ &\quad\times\left[\frac{Q^2\rho(1-\rho)}{\tau(1-\tau)}\right]^{-1/2+i\nu}.\end{aligned} \tag{6.13}$$

https://doi.org/10.1017/9781009290111.008 Published online by Cambridge University Press

Putting all this together we obtain the result that

$$F_2(x,Q^2) = \left(\frac{Q^2}{\mu^2}\right)^{1/2} \frac{\mathcal{N}_g \alpha_s}{8\pi} \sum e_q^2 \int_0^1 d\rho \int_0^1 d\tau \int_{-\infty}^{\infty} d\nu$$
$$\times \frac{1}{\cosh \pi\nu} \left(\frac{Q^2}{\mu^2}\right)^{i\nu} \exp\left(\bar{\alpha}_s \chi_0(\nu) \ln 1/x\right)$$
$$\times \left[1 - 2\rho(1-\rho) - 2\tau(1-\tau) + 12\tau\rho(1-\tau)(1-\rho)\right]$$
$$\times \left[\frac{\rho(1-\rho)}{\tau(1-\tau)}\right]^{-1/2+i\nu} \frac{\Gamma(\delta - 1/2 - i\nu)\Gamma(1/2+i\nu)}{\tau(1-\tau)\Gamma(\delta)}. \qquad (6.14)$$

We can perform the ν-integral by expanding about the saddle point† at $\nu \approx 0$. This has the effect of decoupling all the δ-dependence and renders the ρ- and τ-integrals purely numerical. Thus we can factorize them into some new (and unknown) constant, $\mathcal{N}_2$. Our final result for $F_2(x,Q^2)$ is therefore

$$F_2(x,Q^2) \approx \mathcal{N}_2 \bar{\alpha}_s \sum e_q^2 \left(\frac{Q^2}{\mu^2}\right)^{1/2} \frac{e^{\omega_0 \ln 1/x}}{\sqrt{\bar{\alpha}_s \ln 1/x}}$$
$$\times \exp\left(-\frac{\ln^2(Q^2/\mu^2)}{56\bar{\alpha}_s \zeta(3) \ln 1/x}\right). \qquad (6.15)$$

In Fig. 6.3, we show a sample of the HERA data collected from e–p collisions at a centre-of-mass energy $\sqrt{s} \approx 300$ GeV. The curves arise from Eq.(6.15). What exactly did we do with Eq.(6.15) in order to produce these curves? The answer to this question highlights the difficulty in making firm predictions for the structure function $F_2(x,Q^2)$. The normalization, $\mathcal{N}_2$, is unknown (it depends on non-perturbative physics through the normalization of the proton impact factor and our *ansatz* for its shape, i.e. δ in our toy model) – so we need to fit it to the data. The scale μ^2 is again of non-perturbative origin. Additionally, we do not know the appropriate value of α_s to take nor do we know the appropriate scale to define the logarithms of energy (i.e. do we take $\ln 1/x$ or $\ln 1/2x$, etc?). These are both problems which originate because we only summed the leading logarithms in energy and can only be improved by going beyond this approximation. For

† A brief introduction to the saddle point method is given in Appendix B to this chapter.

https://doi.org/10.1017/9781009290111.008 Published online by Cambridge University Press

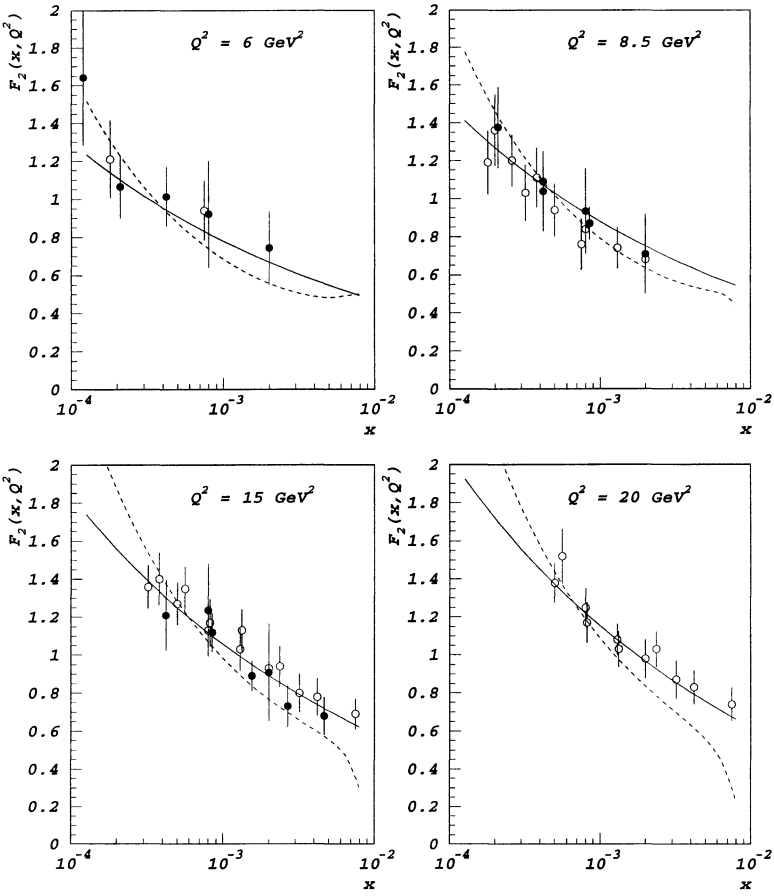

Fig. 6.3. Data on the deep inelastic structure function, $F_2(x, Q^2)$, collected by the H1 (open circles) (Ahmed *et al.* (1995)) and Zeus (full circles) (Derrick *et al.* (1995)) collaborations at the HERA e–p collider.

the solid line we chose $\alpha_s = 0.1$ and introduced a parameter, x_0, such that all occurrences of $\ln 1/x$ are replaced by $\ln x_0/x$. The parameters x_0, $\mathcal{N}_2$ and μ^2 were then fitted to the data. The best fit values were $x_0 = 0.6$, $\mathcal{N}_2 = 0.30$ and $\mu^2 = 0.31$ GeV^2. The ambiguity in x_0 is equivalent to saying that we really cannot answer the question "how low in x must we be to observe the dynamics associated with the leading logarithm summation?", since this

https://doi.org/10.1017/9781009290111.008 Published online by Cambridge University Press

region is defined to be that for which $x \ll x_0$. Correspondingly, we fitted only to data which satisfy this criterion, i.e. we fitted to data with $x < 10^{-2}$. Even so, with this four parameter fit, we are able to obtain good agreement with the low-x data. The dashed line illustrates the strong sensitivity to our choice of α_s. It is produced with $\alpha_s = 0.2$. The other parameters are correspondingly re-fitted, i.e. $x_0 = 0.01$, $\mu^2 = 2$ GeV^2 and $\mathcal{N}_2 = 0.38$, and the fit is to all those data with $x < 10^{-3}$. Since $\omega_0 \propto \alpha_s$ drives the low-x rise we should not be surprised to see a much steeper behaviour with $\alpha_s = 0.2$.

We took a model for the proton impact factor (Eq.(6.10)) which (after dividing by $\mathbf{k}^2$) is peaked in the region of low $\mathbf{k}^2$. In light of the discussion in Section 5.1 of the preceding chapter, we should question the validity of our calculation. The diffusion 'cigar' is tilted (one end fixed by $\sim Q^2$ and the other by $\sim \mu^2$) and as a result there is the danger that contributions from the infra-red region could possibly be large. At the end of this chapter, when we make the connection with the Altarelli–Parisi approach, we shall show that (neglecting terms suppressed by powers of $\sim \mu^2/Q^2$) the largely unknown infra-red physics factorizes from the known perturbative physics. This is good news since it means that we can make meaningful perturbative calculations. We defer further studies on the total inelastic cross-section to the end of this chapter and turn to a process which avoids many of the problems associated with the unknown infra-red effects we have just been discussing.

6.3 Associated jet production

Although the total deep inelastic cross-section is relatively straightforward to measure, the work of the last section has taught us that the non-perturbative behaviour of the proton impact factor spoils a clean perturbative analysis. Our problem was with the fact that the proton impact factor introduced unknown non-perturbative effects into our calculation. We modelled them at the price of introducing unknown parameters μ^2 and δ. If we could replace this impact factor with one which is peaked at a much larger scale then we eliminate most of our difficulties (we always need to worry about the effects of diffusion if the centre-of-mass energy is

https://doi.org/10.1017/9781009290111.008 Published online by Cambridge University Press

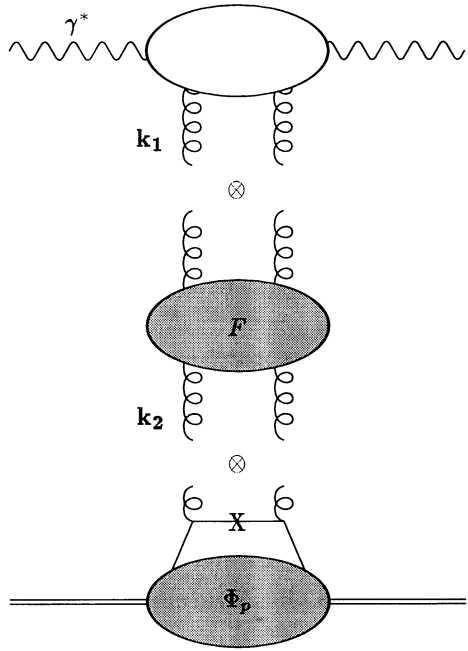

Fig. 6.4. One of the amplitudes relevant for associated jet production. The lower quark line could also be a gluon line and the 'X' denotes a high-p_T parton.

too big). Mueller (1991) appreciated that it is possible to do this by insisting on the production of a high-p_T parton which emerges at a small angle relative to the direction of the incoming proton (e.g. in the $\gamma^* p$ CM frame). In Fig. 6.4 we show the relevant amplitude. The cross on the lower parton line indicates that it has a high transverse momentum. The initial studies into associated jet production can be found in the papers by Kwiecinski, Martin & Sutton (1992), Bartels, De Roeck & Loewe (1992) and Tang (1992).

We say that the high-p_T parton is in the forward direction, i.e. it carries a not-too-small fraction, x_j, of the incoming proton energy (relative to its transverse momentum). Of course, experimentalists do not measure this parton. They observe the jet of hadrons which it produces. In this limit, we may neglect the transverse

https://doi.org/10.1017/9781009290111.008 Published online by Cambridge University Press

momentum of the parton from the proton. Consequently, if the associated jet is a quark of flavour i, the proton impact factor, Φ_p^i, becomes

$$\Phi_p^i(\mathbf{k_2}) = 8\pi^2\alpha_s q_i(x_j, \mathbf{k_2^2}), \tag{6.16}$$

i.e. the quark impact factor of Eq.(4.37) multiplied by the quark number density. The colour factor for this process is now $\mathcal{G} = NG_0^{(1)}$ (since we do not average over the colour of the quark loop in the photon impact factor). Putting the number of colours equal to 3 (as we shall do subsequently in this chapter), $\mathcal{G} = \frac{2}{3}$. Similarly,

$$\Phi_p^g(\mathbf{k_2}) = 8\pi^2\alpha_s g(x_j, \mathbf{k_2^2}), \tag{6.17}$$

for a gluon jet and the colour factor is now $\frac{1}{8}f_{abc}f_{abd}\mathrm{Tr}(\tau_c\tau_d) = \frac{3}{2}$, i.e. it is $C_2(A)/C_2(F) = \frac{9}{4}$ larger than the quark colour factor.

By observing the associated jet, we fix $\mathbf{k_2} = \mathbf{k_j}$ (assuming the incoming parton to be collinear with the proton). Thus, for the differential structure functions we can write:

$$x_j\mathbf{k_j^2}\frac{\partial^2 F_\lambda(x, Q^2; x_j, \mathbf{k_j^2})}{\partial x_j \partial \mathbf{k_j^2}} = \frac{Q^2}{4\pi^2\alpha}8\pi^2\alpha_s\frac{3}{2}\frac{\pi}{(2\pi)^4}$$

$$\times \int \frac{d^2\mathbf{k}}{\mathbf{k}^2}\Phi_\lambda(\mathbf{k})F(x/x_j, \mathbf{k}, \mathbf{k_j})\left[G(x_j, \mathbf{k_j^2}) + \frac{4}{9}\Sigma(x_j, \mathbf{k_j^2})\right], \tag{6.18}$$

where

$$\begin{aligned} G(x, Q^2) &\equiv xg(x, Q^2) \quad \text{and} \\ \Sigma(x, Q^2) &\equiv \sum_{i=1}^{n_f}[xq_i(x, Q^2) + x\bar{q}_i(x, Q^2)] \end{aligned} \tag{6.19}$$

are the momentum distribution functions. Notice that we have taken x/x_j in the arguments of F. Since $x_j \gg x$ this is, strictly speaking, sub-leading. However our choice reflects the fact that the γ^*–parton sub-energy is $\approx Q^2(x_j/x)$.

By looking at forward jets, i.e. $x_j \sim 1$ and $\mathbf{k_j^2} \sim Q^2$, we are focusing on a region where the parton densities, $G(x_j, \mathbf{k_j^2})$ and $\Sigma(x_j, \mathbf{k_j^2})$, are experimentally well measured. In this way we have avoided any need to invoke non-perturbative effects directly since they have been implicitly factorized into the parton density functions.

Let us focus on the scattering of transverse photons, the impact factor is given in Eq.(A.6.21) of Appendix A to this chapter. Again

https://doi.org/10.1017/9781009290111.008 Published online by Cambridge University Press

we can perform the $\mathbf{k}$-integral (using Eq.(6.13)). Keeping only the $n = 0$ term in the BFKL expansion it then follows that

$$x_j \mathbf{k}_\mathbf{j}^2 \frac{\partial^2 F_T(x, Q^2; x_j, \mathbf{k}_\mathbf{j}^2)}{\partial x_j \partial \mathbf{k}_\mathbf{j}^2} = \frac{\pi \bar{\alpha}_s^2}{3} \left[G(x_j, \mathbf{k}_\mathbf{j}^2) + \frac{4}{9} \Sigma(x_j, \mathbf{k}_\mathbf{j}^2) \right]$$
$$\times \sum_{q=1}^{n_f} e_q^2 \int_{-\infty}^{\infty} \frac{d\nu}{8\pi} \frac{1}{\cosh \pi\nu} \int \frac{d\rho d\tau}{\tau(1-\tau)}$$
$$\times [\tau^2 + (1-\tau)^2][\rho^2 + (1-\rho)^2] \left[\frac{\rho(1-\rho)}{\tau(1-\tau)} \right]^{-1/2+i\nu}$$
$$\times \left(\frac{Q^2}{\mathbf{k}_\mathbf{j}^2} \right)^{1/2+i\nu} \exp\left(\bar{\alpha}_s \chi_0(\nu) \ln(x_j/x) \right). \tag{6.20}$$

Performing the ν-integral by the saddle point method about $\nu = 0$ and using

$$\int_0^1 d\rho \, \frac{\rho^2 + (1-\rho)^2}{\sqrt{\rho(1-\rho)}} = \frac{3\pi}{4}, \tag{6.21}$$

gives

$$x_j \mathbf{k}_\mathbf{j}^2 \frac{\partial^2 F_T(x, Q^2; x_j, \mathbf{k}_\mathbf{j}^2)}{\partial x_j \partial \mathbf{k}_\mathbf{j}^2} \approx \left[G(x_j, \mathbf{k}_\mathbf{j}^2) + \frac{4}{9} \Sigma(x_j, \mathbf{k}_\mathbf{j}^2) \right]$$
$$\times \bar{\alpha}_s A_T \sum_{q=1}^{n_f} e_q^2 \left(\frac{\pi \bar{\alpha}_s}{126 \zeta(3) \ln(x_j/x)} \right)^{1/2} \left(\frac{Q^2}{\mathbf{k}_\mathbf{j}^2} \right)^{1/2}$$
$$\times \left(\frac{x_j}{x} \right)^{\omega_0} \exp\left(- \frac{\ln^2(Q^2/\mathbf{k}_\mathbf{j}^2)}{56 \zeta(3) \bar{\alpha}_s \ln(x_j/x)} \right), \tag{6.22}$$

where $A_T = 9\pi^2/128$.

In the case of longitudinal photons the calculation proceeds along similar lines and it is straightforward to show that the form is just as for transverse photons, but with A_T replaced by $A_L = \pi^2/64$. Since $F_2(x, Q^2) = F_L(x, Q^2) + F_T(x, Q^2)$, we have $A_2 = 11\pi^2/128$.

We have suggested that $\mathbf{k}_\mathbf{j}^2$ should be chosen to be $\sim Q^2$. This has the clear benefit (provided $Q^2 \gg \Lambda_{QCD}^2$) of ensuring that there is no danger of diffusion effects forcing the loop integrals (which are implicit in the BFKL amplitude, $F(x_j/x, k^2, \mathbf{k}_\mathbf{j}^2)$) to

https://doi.org/10.1017/9781009290111.008 Published online by Cambridge University Press

pick up large contributions from the infra-red region. In the language of Section 5.1, the axis of the diffusion 'cigar' is horizontal and well above the dangerous small τ' region. However, since the effect of diffusion increases with increasing x_j/x there is a limit to how low in x we can go before non-perturbative effects start to become important in the calculation of the BFKL amplitude, i.e. the diffusion 'cigar' becomes too fat. For a more detailed discussion on the effects of diffusion we refer to the paper by Bartels & Lotter (1993).

One other advantage of choosing $\mathbf{k}_\mathbf{j}^2 \sim Q^2$ arises once we appreciate that the $\ln 1/x$ terms that we have been concentrating so hard on summing up are not the only logarithms that can be large. There are also $\ln Q^2$ terms which can compete in the deep inelastic regime. The Altarelli–Parisi equations tell us how to sum the $\ln Q^2$ terms which occur in the perturbative expansion. These terms compete with the $\ln 1/x$ terms and ideally we should look at both series in a complete treatment. However, by picking $\mathbf{k}_\mathbf{j}^2 \sim Q^2$ we ensure that there are no large logarithms in Q^2 in the BFKL amplitude (only $\ln Q^2/\mathbf{k}_\mathbf{j}^2$ terms appear). The summation of the large $\ln \mathbf{k}_\mathbf{j}^2$ logarithms is implicit in the parton densities, $G(x_j, \mathbf{k}_\mathbf{j}^2)$ and $\Sigma(x_j, \mathbf{k}_\mathbf{j}^2)$, which, as we have said, we are able to read off from experiment.

Let us conclude our discussion of the associated jet process with a short study of the feasibility of its experimental detection. The main difficulty associated with insisting on seeing a forward jet arises precisely because the jet is *forward*. There is a limit to how forward the jet can go, since we need it to appear in the detector (i.e. not vanish down the beam-pipe). Also, since there are other particles heading down the forward beam-pipe (from the break up of the proton) our jet had better be sufficiently well collimated and isolated. If Θ is the minimum angle at which the parton can emerge (in the lab frame) so that the associated jet is observable, i.e. it appears as a discernible jet in the detectors, then it follows that

$$\frac{\sqrt{\mathbf{k}_\mathbf{j}^2}}{x_j p} > \tan\Theta.$$

In addition, the high energy limit demands that $x/x_j \ll 1$. So we

https://doi.org/10.1017/9781009290111.008 Published online by Cambridge University Press

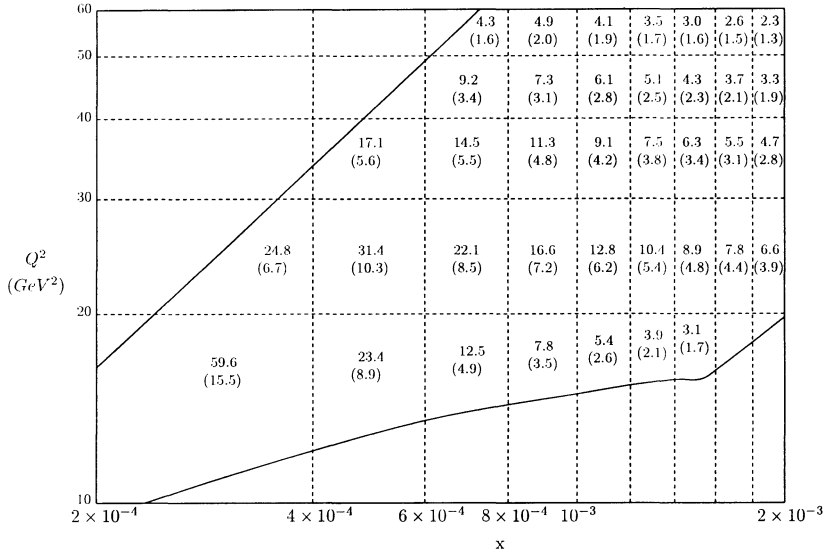

Fig. 6.5. Cross-section for the associated jet process. The cross-sections are in pb.

have competing constraints which lead to important cuts on the allowed phase space. These problems are inherently due to the configuration of the experiment (and the existence of a proton remnant) and cannot be circumvented simply by increasing the proton beam momentum (since this makes the jet more forward) nor by increasing the electron beam momentum (since we need to detect the scattered electron). In Fig. 6.5, cross-sections for the associated jet process are shown in different $x - Q^2$ bins. The HERA collider is used to define the proton (820 GeV) and electron (30 GeV) lab frame energies and the typical acceptance cuts. The boundary lines are due to the cuts on the angle of the scattered electron and the cross-sections are computed with the following kinematical constraints: $\Theta = 5^\circ$, $x_j > 0.05$, $x_j/x > 10$, $Q^2/2 < \mathbf{k_j^2} < 2Q^2$. The numbers in parentheses are the cross-sections calculated without BFKL corrections, i.e. $F(s, \mathbf{k_1}, \mathbf{k_2}, \mathbf{0}) = \delta^2(\mathbf{k_1} - \mathbf{k_2})$. We took these results from the paper by Martin, Kwiecinski & Sutton (1992).

https://doi.org/10.1017/9781009290111.008 Published online by Cambridge University Press

6.4 The Altarelli–Parisi approach

In most introductory text books on QCD one will find a discussion of the quark–parton model of the proton. The impulse approximation allows us to consider (in the infinite momentum frame) the proton as a system of partons whose transverse motion is frozen over the time scales typical of the interaction with the off-shell photon. The partons are point-like and so we are led to the concept of Bjorken scaling, i.e. the Q^2-independence of the deep inelastic structure function, $F_2(x, Q^2)$, and the vanishing of the longitudinal cross-section (the Callan-Gross relation) in the $Q^2 \to \infty$ limit.

The experimental data is consistent with this picture to a fair approximation but scaling violations are seen. These violations can be accounted for within the framework of QCD perturbation theory using the so-called Altarelli–Parisi equations. Subsequently, we will refer to these equations more correctly as the **DGLAP equations**, after Dokshitzer (1977), Gribov & Lipatov (1972) and Altarelli & Parisi (1977). The DGLAP equations rely on the notion of proton quark, $q_i(x, Q^2)$, and gluon, $g(x, Q^2)$, density functions which specify the number density of partons within the proton. For example, the first moment of the quark density (summed over all quark flavours) is to be interpreted as the fraction of the proton's momentum carried by the quarks, i.e.

$$\int_0^1 dx[\Sigma(x, Q^2) + G(x, Q^2)] = 1,$$

where $G(x, Q^2)$ and $\Sigma(x, Q^2)$ are defined as in Eq.(6.19).

Let us recall[†] the DGLAP equations:

$$\frac{\partial}{\partial \ln Q^2} \begin{pmatrix} \Sigma(x, Q^2) \\ G(x, Q^2) \end{pmatrix} = \frac{\alpha_s}{2\pi} \int_x^1 dz \begin{pmatrix} P_{qq}(z) & 2n_f P_{qg}(z) \\ P_{gq}(z) & P_{gg}(z) \end{pmatrix} \begin{pmatrix} \Sigma(x/z, Q^2) \\ G(x/z, Q^2) \end{pmatrix}. \quad (6.23)$$

These equations are easiest to solve in moment space, i.e. we take the Mellin transforms of the parton densities using the fact that

[†] For an introduction to the DGLAP formalism, we refer to the standard texts, e.g. Field (1989), Halzen & Martin (1984), Greiner & Schäfer (1994), Roberts (1990).

https://doi.org/10.1017/9781009290111.008 Published online by Cambridge University Press

for Q^2 fixed, $s \propto 1/x$. Accordingly we define

$$\begin{pmatrix} \Sigma_N(Q^2) \\ G_N(Q^2) \end{pmatrix} = \int_0^1 dx x^{N-1} \begin{pmatrix} \Sigma(x,Q^2) \\ G(x,Q^2) \end{pmatrix}, \qquad (6.24)$$

$$\gamma_{ij}^N = \frac{\alpha_s}{2\pi} \int_0^1 dz z^N P_{ij}(z).$$

The moment index, N, is not to be confused with the number of colours! Although in preceding chapters we labelled the moment index ω, in this chapter we adopt the notation which is most common in the literature when discussing the deep inelastic structure functions. The DGLAP equations now reduce to a pair of simultaneous equations:

$$\frac{\partial}{\partial \ln Q^2} \begin{pmatrix} \Sigma_N(Q^2) \\ G_N(Q^2) \end{pmatrix} = \begin{pmatrix} \gamma_{qq}^N & 2n_f\gamma_{qg}^N \\ \gamma_{gq}^N & \gamma_{gg}^N \end{pmatrix} \begin{pmatrix} \Sigma_N(Q^2) \\ G_N(Q^2) \end{pmatrix}. \qquad (6.25)$$

This is easy to see after inserting a Dirac delta function to write

$$\int_x^1 dz P_{ij}(z) f(x/z) = \int_0^1 dz \int_0^1 dy\, z P_{ij}(z) f(y) \delta(x - yz).$$

The solution is now straightforward to obtain. The matrix, γ_{ij}^N, is called the **anomalous dimension** matrix (for reasons that will become clear) and is calculable in perturbation theory.

In terms of the parton densities the deep inelastic structure functions can be written in the simple form:

$$F_{\lambda,N}(Q^2) = \sum_i e_i^2 C_{i,N}^{(\lambda)}(Q^2/\mu_F^2, \alpha_s(\mu_F^2)) Q_{i,N}(\mu_F^2)$$
$$+ \; C_{g,N}^{(\lambda)}(Q^2/\mu_F^2, \alpha_s(\mu_F^2)) G_N(\mu_F^2), \qquad (6.26)$$

where $Q_{i,N}(\mu_F^2)$ is the Nth moment of $xq_i(x,\mu_F^2)$. The coefficient functions, $C_{(i,g),N}^{(\lambda)}$, are computable in perturbation theory, i.e. all the long distance physics factorizes into the parton densities. The factorization scale, μ_F^2, is arbitrary and the final result does not depend upon it to the given order (in α_s) of the calculation, i.e. the μ_F^2-dependence is sub-leading in α_s. It is usually best to take $\mu_F^2 = Q^2$, so that terms $\sim \alpha_s(\mu_F^2) \ln Q^2/\mu_F^2$ do not appear in the coefficient functions but are absorbed into the parton densities. This factorization of long- and short-distance physics is a fundamental and very important ingredient of QCD. The parton density functions are universal, e.g. the cross-section for Drell–Yan production of muon pairs in hadron–hadron colliders can be written

https://doi.org/10.1017/9781009290111.008 Published online by Cambridge University Press

as a product of two parton density functions (one for each hadron) and a hard sub-process cross-section (i.e. $q\bar{q} \to \mu^+\mu^-$). The parton densities are just those which appear in the deep inelastic structure functions. Factorization is proven only for the 'leading twist' component of the matrix elements (we refer to the review by Collins, Soper & Sterman (1989) and references therein for further details). In the case of the deep inelastic structure functions this means that factorization applies to the cross-section after we have thrown away all terms which vanish as $Q^2 \to \infty$.

By way of illustration let us consider the Nth moment of the structure function $F_{2,N}(Q^2)$. In the lowest order of perturbation theory, the gluon coefficient function vanishes (since the gluon carries no electromagnetic charge) and the quark coefficient functions are simply unity, i.e.

$$F_2(x,Q^2) = \sum_{i=1}^{n_f} e_i^2 x[q_i(x,Q^2) + \bar{q}_i(x,Q^2)]. \tag{6.27}$$

The quark densities are obtained by solving the DGLAP equations with the lowest order splitting functions, i.e.

$$\begin{aligned}
\gamma_{qq}^N &= \frac{\bar{\alpha}_s}{9}\left(\frac{2}{(N+1)(N+2)} - 1 - 4\sum_{j=2}^{N+1}\frac{1}{j}\right), \\
\gamma_{qg}^N &= \frac{\bar{\alpha}_s}{12}\frac{N^2+3N+4}{(N+1)(N+2)(N+3)}, \\
\gamma_{gq}^N &= \frac{2\bar{\alpha}_s}{9}\frac{N^2+3N+4}{N(N+1)(N+2)}, \\
\gamma_{gg}^N &= -\frac{\bar{\alpha}_s}{2}\left(\frac{(N-1)(N+2)}{N(N+1)} + \frac{(N-1)(N+6)}{6(N+2)(N+3)}\right. \\
&\qquad \left. + \sum_{j=3}^{N+1}\frac{2}{j} + \frac{1}{9}n_f\right).
\end{aligned} \tag{6.28}$$

To solve Eq.(6.25), we need to fix the boundary conditions by specifying the parton densities at some scale, μ^2. The solution then gives the parton densities at all other scales. The parton densities which are obtained as the solution to Eq.(6.25), which is obtained using the (lowest order) anomalous dimensions of Eq.(6.28), include all perturbative corrections to the inputs ($q(x,\mu^2)$ and

https://doi.org/10.1017/9781009290111.008 Published online by Cambridge University Press

$g(x,\mu^2)$) which are $\sim (\alpha_s(\mu_F^2)\ln \mu_F^2/\mu^2)^n$, i.e. the corrections are computed to leading $\ln Q^2$ accuracy. At the next order (i.e. including those terms which are $\sim \alpha_s^2$ in the anomalous dimension matrix and $\sim \alpha_s$ in the coefficient functions) the DGLAP equations sum the next-to-leading logarithms, $\sim \alpha_s(\mu_F^2)(\alpha_s(\mu_F^2)\ln \mu_F^2/\mu^2)^n$.

Provided we take Q^2 large enough (so that the leading twist terms dominate) then we expect to be able to factorize the non-perturbative behaviour of the BFKL amplitude and to re-write it in a way which is consistent with the low-x limit of the DGLAP formalism. Let us now investigate how this comes about.

We start with the unintegrated gluon density of Eq.(6.5). It will be useful to introduce the variables γ and N which are the Mellin conjugates to $\mathbf{k}^2$ and x, respectively, i.e.

$$\begin{aligned} \mathcal{F}_N(\mathbf{k}) &= \int_0^1 dx x^{N-1}\mathcal{F}(x,\mathbf{k}), \\ \tilde{\mathcal{F}}_N(\gamma) &= \int_1^\infty d\left(\frac{\mathbf{k}^2}{\mu^2}\right)\left(\frac{\mathbf{k}^2}{\mu^2}\right)^{-\gamma-1}\mathcal{F}_N(\mathbf{k}). \end{aligned} \tag{6.29}$$

Equation (6.29) can be inverted using

$$\mathcal{F}_N(\mathbf{k}) = \int_{1/2-i\infty}^{1/2+i\infty}\frac{d\gamma}{2\pi i}\left(\frac{\mathbf{k}^2}{\mu^2}\right)^\gamma \tilde{\mathcal{F}}_N(\gamma). \tag{6.30}$$

With these definitions, we thus have

$$\begin{aligned} \mathcal{F}_N(\mathbf{k}) &= \frac{1}{(2\pi)^3}\int\frac{d^2\mathbf{k}'}{\pi\mathbf{k}'^2}\Phi_p(\mathbf{k}')\int_{1/2-i\infty}^{1/2+i\infty}\frac{d\gamma}{2\pi i} \\ &\quad\times\left(\frac{\mathbf{k}^2}{\mathbf{k}'^2}\right)^\gamma\frac{1}{N-\bar{\alpha}_s\chi(\gamma)}. \end{aligned} \tag{6.31}$$

As usual, we have kept only the $n=0$ term. Also, we substituted γ for $1/2+i\nu$ and defined $\chi(\gamma)\equiv\chi_0(\nu)$. Using Eq.(4.27) this means that

$$\chi(\gamma) = -2\gamma_E - \psi(\gamma) - \psi(1-\gamma).$$

The $\mathbf{k}'$-integral can be performed (it simply takes the Mellin transform of the proton impact factor). Thus,

$$\mathcal{F}_N(\mathbf{k}) = \frac{1}{(2\pi)^3}\int_{1/2-i\infty}^{1/2+i\infty}\frac{d\gamma}{2\pi i}\tilde{\Phi}_p(\gamma,\mu)\left(\frac{\mathbf{k}^2}{\mu^2}\right)^\gamma\frac{1}{N-\bar{\alpha}_s\chi(\gamma)}. \tag{6.32}$$

https://doi.org/10.1017/9781009290111.008 Published online by Cambridge University Press

Equivalently, we may write

$$\tilde{\mathcal{F}}_N(\gamma) = \tilde{\mathcal{F}}_N^0(\gamma,\mu)\frac{N}{N-\bar{\alpha}_s\chi(\gamma)}, \tag{6.33}$$

where

$$\tilde{\mathcal{F}}_N^0(\gamma,\mu) = \frac{1}{(2\pi)^3}\frac{\Phi_p(\gamma,\mu)}{N} \tag{6.34}$$

is the (double Mellin transform of the) unintegrated gluon density in the absence of any QCD corrections.

So far we have merely repeated the work discussed earlier in this chapter, albeit in a different notation. The moments of the structure functions $F_{i,N}(Q^2)$ also take on simple forms in this notation. Concentrating on $F_{2,N}(Q^2)$ we have

$$F_{2,N}(Q^2) = \frac{\pi\bar{\alpha}_s}{12}\sum_{q=1}^{n_f} e_q^2 \int \frac{d\gamma}{2\pi i}\tilde{\mathcal{F}}_N(\gamma)\int_0^1 \frac{d\rho\, d\tau}{\sin\pi\gamma}\left(\frac{Q^2}{\mu^2}\right)^\gamma \tag{6.35}$$

$$\times \left[\frac{\rho(1-\rho)}{\tau(1-\tau)}\right]^\gamma \frac{1-2\rho(1-\rho)-2\tau(1-\tau)+12\rho(1-\rho)\tau(1-\tau)}{\rho(1-\rho)}.$$

To obtain this result, we needed to use Eq.(6.13) to perform the $\mathbf{k}'^2$ integral. The ρ and τ integrals can also be done (they are standard integrals) and yield

$$F_{2,N}(Q^2) = \int \frac{d\gamma}{2\pi i}\frac{h_{2,N}(\gamma)}{\gamma^2}\tilde{\mathcal{F}}_N(\gamma)\left(\frac{Q^2}{\mu^2}\right)^\gamma, \tag{6.36}$$

where

$$h_{2,N}(\gamma) = \frac{\pi\bar{\alpha}_s}{24}\sum_{q=1}^{n_f} e_q^2 \frac{\pi\gamma}{\sin\pi\gamma}\frac{\Gamma(1+\gamma)\Gamma(1-\gamma)}{\Gamma(3/2+\gamma)\Gamma(3/2-\gamma)}\frac{2+3\gamma-3\gamma^2}{3-2\gamma}.$$

We are then left with only the integral over γ to perform.

The leading twist behaviour is specified by those contributions which do not vanish as $Q^2/\mu^2 \to \infty$. Since $Q^2 > \mu^2$, we need to close the γ-plane contour in the left half plane. There are two poles which lead to finite contributions as $Q^2/\mu^2 \to \infty$:
(a) the pole $\bar{\gamma} > 0$ which satisfies $N = \bar{\alpha}_s\chi(\bar{\gamma})$;
(b) the pole at $\gamma = 0$ (it is only a simple pole since $\chi(\gamma) \sim 1/\gamma$ as $\gamma \to 0$).
All other poles (which occur for negative integer values of γ) lead to contributions which are suppressed by powers of μ^2/Q^2. The pole at $\gamma = 0$ leads to a scaling (i.e. Q^2-independent) contribution

https://doi.org/10.1017/9781009290111.008 Published online by Cambridge University Press

and can be absorbed into the input quark density. Thus to reveal the predicted scaling violations we focus on $\partial F_{2,N}(Q^2)/\partial \ln Q^2$.

$$\frac{\partial F_{2,N}(Q^2)}{\partial \ln Q^2} = h_{2,N}(\bar{\gamma}) R_N \mathcal{F}_N^0(\bar{\gamma}) \left(\frac{Q^2}{\mu^2}\right)^{\bar{\gamma}}, \qquad (6.37)$$

where

$$R_N = \frac{1}{-\bar{\alpha}_s \bar{\gamma} \chi'(\bar{\gamma})/N}.$$

In order to obtain the leading behaviour at low x of $F_2(x, Q^2)$ we examine this moment equation near $N = \omega_0$ for which

$$\lim_{N \to \omega_0} R_N = -\frac{\omega_0}{\sqrt{14 \bar{\alpha}_s \zeta(3)(N - \omega_0)}}$$

and

$$\lim_{N \to \omega_0} \bar{\gamma} = \frac{1}{2} - \sqrt{\frac{N - \omega_0}{14 \bar{\alpha}_s \zeta(3)}}.$$

In this approximation Eq.(6.37) is the Mellin transform of Eq.(6.15). It is important to note that the leading $x^{-\omega_0}$ behaviour arises from the singularity in R_N and is present for *any value of* Q^2. A similar growth at low x arises from the factor $(Q^2/\mu^2)^{\bar{\gamma}}$ but this is only important for $Q^2 \gg \mu^2$.

Furthermore we see from Eq.(6.37) that deviations from Bjorken scaling are present even in the limit of asymptotically large Q^2. The size of these 'anomalous' scaling violations is determined by $\bar{\gamma}$. Accordingly, we call this the **BFKL anomalous dimension** and soon we will show that it is equal to the DGLAP gluon anomalous dimension, γ_{gg}^N (in the low-x, i.e. small-N, limit). From the fact that $\chi(\bar{\gamma}) = N/\bar{\alpha}_s$ and using (for $|\gamma| < 1$)

$$\chi(\gamma) = \frac{1}{\gamma} + 2 \sum_{r=1}^{\infty} \zeta(2r+1) \gamma^{2r},$$

we can obtain the perturbative expansion of $\bar{\gamma}$:

$$\bar{\gamma} = \frac{\bar{\alpha}_s}{N} + 2\zeta(3) \left(\frac{\bar{\alpha}_s}{N}\right)^4 + 2\zeta(5) \left(\frac{\bar{\alpha}_s}{N}\right)^6 + \mathcal{O}\left(\frac{\bar{\alpha}_s}{N}\right)^7. \qquad (6.38)$$

We are now ready to make the explicit connection with the DGLAP result. At low x, we are not sensitive to the valence quarks so the q and $\bar{q}$ distributions in the proton are equal. Also, in the BFKL treatment we ignored intrinsic quark densities, so we must

https://doi.org/10.1017/9781009290111.008 Published online by Cambridge University Press

drop all terms $\propto \Sigma_N(Q^2)$. Finally, the $\ln Q^2$ derivative of the coefficient functions is sub-leading. Equation (6.26) then becomes

$$\frac{\partial F_{2,N}(Q^2)}{\partial \ln Q^2} = (\langle e_q^2 \rangle 2n_f \gamma_{qg}^N + C_g^N(1, \alpha_s)) G_N(Q^2), \tag{6.39}$$

where

$$\frac{\partial G_N(Q^2)}{\partial \ln Q^2} = \gamma_{gg}^N G_N(Q^2). \tag{6.40}$$

For fixed coupling this means that

$$G_N(Q^2) = G_N(\mu^2) \left(\frac{Q^2}{\mu^2} \right)^{\gamma_{gg}^N}. \tag{6.41}$$

Thus, for consistency with Eq.(6.37), $\gamma_{gg}^N = \bar{\gamma}$. Note that the equivalence of the first term in the expansions (in $\bar{\alpha}_s/N$) of γ_{gg}^N and $\bar{\gamma}$ can be seen explicitly by comparing Eq.(6.38) with the $N \to 0$ limit of Eq.(6.28). In addition, we also require that

$$(\langle e_q^2 \rangle 2n_f \gamma_{qg}^N + C_g^N(1, \alpha_s)) G_N(\mu^2) = h_{2,N} R_N \mathcal{F}_N^0(\bar{\gamma}, \mu). \tag{6.42}$$

To summarize, we have shown that the leading twist part of the BFKL solution for the structure function factorizes in a manner consistent with the DGLAP approach. The equivalence of the (leading-twist) BFKL solution and the $N \to 0$ limit of the DGLAP solution allows us to identify the DGLAP gluon anomalous dimension, γ_{gg}^N, with the BFKL anomalous dimension, $\bar{\gamma}$ (calculated to all orders in $\bar{\alpha}_s/N$). The equivalence also allows us to identify the DGLAP coefficient functions with the BFKL 'coefficient function' as in Eq.(6.42). However, there is an ambiguity in extracting the coefficient function which we shall now examine.

In the lowest order of perturbation theory, $\bar{\gamma} = \bar{\alpha}_s/N$, $R_N = 1$, $h_{2,N} = \bar{\alpha}_s \langle e_q^2 \rangle n_f/9$ and $\gamma_{qg}^N = \bar{\alpha}_s/18$. To this order, Eq.(6.39) reduces to

$$\frac{\partial F_{2,N}(Q^2)}{\partial \ln Q^2} = \sum_{q=1}^{n_f} e_q^2 \frac{\bar{\alpha}_s}{9} G_N(Q^2). \tag{6.43}$$

Comparing with Eq.(6.9), we see that (at this lowest order) the BFKL gluon density defined by Eq.(6.6) is precisely the DGLAP gluon density. Also, comparison with Eq.(6.37) forces us to identify

$$G_N(\mu^2) = \mathcal{F}_N^0(\bar{\gamma}, \mu).$$

https://doi.org/10.1017/9781009290111.008 Published online by Cambridge University Press

However, beyond the lowest order R_N starts to deviate from unity. Since we do not know the scale at which to evaluate α_s we have the freedom to either: absorb all or part of R_N into the input density, $G_N(\mu^2)$, or absorb all or part of R_N into the definition of $\langle e_q^2 \rangle 2n_f \gamma_{qg}^N + C_g^N(1, \alpha_s)$. This ambiguity is a factorization scheme ambiguity and is a direct result of the leading logarithmic nature of the calculation.

We know, from the standard renormalization group approach, that it is appropriate to evaluate the anomalous dimensions at the scale Q^2 in the DGLAP evolution. This then forces us to make the replacement,

$$\left(\frac{Q^2}{\mu^2}\right)^{\bar{\gamma}} \to \exp \int_{\mu^2}^{Q^2} \frac{dq^2}{q^2} \bar{\gamma}(q^2) \tag{6.44}$$

and we have made explicit the fact that $\bar{\gamma}$ should be evaluated at $\alpha_s(q^2)$ on the right hand side. Similarly, we evaluate the coefficient function at $\alpha_s(Q^2)$, i.e. $h_{2,N}(Q^2)$. The scheme ambiguity is still present in R_N, so we have no guidance as to what scale to evaluate it at. The replacement of Eq.(6.44) arises as a result of the radiative corrections which cause the QCD coupling to run. As such it is formally beyond the leading BFKL approximation. For a more detailed investigation of factorization in the high energy regime see the paper by Catani & Hautmann (1994).

6.5 Exclusive distributions and coherence

The derivation of the BFKL equation presented in Chapters 3 and 4 relies upon the validity of the Regge kinematics (i.e. strong ordering in the Sudakov variables). It turns out that this kinematic regime is generally only applicable for the calculation of elastic-scattering cross-sections (and hence total cross-sections), which is where we have been using it hitherto.

In this section we would like to generalize the multi-Regge kinematics so as to allow the calculation of more exclusive quantities, e.g. the number of gluons emitted in deep inelastic scattering. This generalization is made by accounting for QCD coherence effects. Here we present only a brief outline of the motivation for coherence in QCD but refer the reader to the wealth of literature (see e.g. Dokshitzer, Khoze, Troyan & Mueller (1991) and references

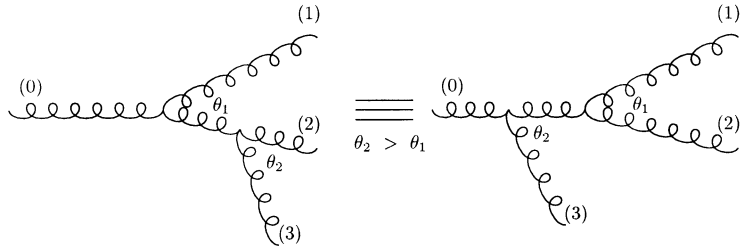

Fig. 6.6. The amplitude for gluon (0) to decay into two gluons (1) and (2) with opening angle θ_1 and for gluon (3) to be radiated off either gluon (1) or gluon (2) (as shown) with opening angle θ_2, where $\theta_2 > \theta_1$, is equivalent to the amplitude for gluon (0) to radiate gluon (3) with opening angle θ_2 and then to decay into gluons (1) and (2).

therein) for a more detailed treatment. We will show that, when accounted for, coherence leads to terms which have additional logarithms (in s) compared to the naive BFKL expectations. These extra logarithms cancel for fully inclusive quantities but not for more exclusive ones (where they provide the dominant contribution). For more details regarding coherence in low-x physics we refer to the work of Ciafaloni (1988), Catani, Fiorani & Marchesini (1990a,b), Catani, Fiorani, Marchesini & Oriani (1991) and Marchesini (1995).

If we consider a time-like (off-shell) parent gluon decaying into two daughter gluons with opening angle θ_1, followed by a further emission of a grand-daughter gluon from one of the daughter gluons with opening angle θ_2, where $\theta_2 > \theta_1$, then at the time of emission the transverse component of the wavelength of the grand-daughter gluon is larger than the transverse spatial separation of the two daughter gluons. In that case the grand-daughter gluon cannot resolve the colours of the individual daughter gluons, but only that of the parent, so that the amplitude for the process is equivalent to the amplitude for the process in which the grand-daughter gluon is emitted directly off the parent, see Fig. 6.6. This is the phenomenon of **colour coherence** and it leads to the angular ordering of sequential gluon emissions in a cascade, i.e. if the opening angle of the ith gluon is θ_i then $\theta_i < \theta_{i-1}$.

https://doi.org/10.1017/9781009290111.008 Published online by Cambridge University Press

In the case of deep inelastic scattering it is convenient to consider successive gluon emission from the target proton, which has zero transverse momentum, up towards the virtual photon, which has momentum $\mathbf{k}$ transverse to the electron–proton system given by

$$\mathbf{k}^2 = Q^2(1-y).$$

Suppose the $(i-1)$th emitted gluon (from the proton) has energy E_{i-1} and that it emits a gluon with a fraction $(1-z_i)$ of this energy and a transverse momentum of magnitude q_i. The (small) opening angle θ_i of this emitted gluon is given approximately by

$$\theta_i \approx \frac{q_i}{(1-z_i)E_{i-1}},$$

where z_i is the fraction of the energy of the $(i-1)$th gluon carried off by the ith gluon, i.e.

$$z_i = \frac{E_i}{E_{i-1}}.$$

Colour coherence leads to angular ordering with increasing opening angles towards the hard scale (the photon) so in this case we have $\theta_{i+1} > \theta_i$, which may be expressed as

$$\frac{q_{i+1}}{(1-z_{i+1})} > \frac{z_i q_i}{(1-z_i)}. \tag{6.45}$$

In the multi-Regge limit where $z_i, z_{i+1} \ll 1$ this reduces to

$$q_{i+1} > z_i q_i. \tag{6.46}$$

For the first emission, we take $q_0 z_0 \equiv \mu$. The kinematics of the virtual graphs (which reggeize the t-channel gluons) is similarly modified and ensures the cancellation of the collinear singularities in inclusive quantities.

In Chapters 2 and 3 we assumed that the transverse momenta of the gluons in the ladder were all of the same order of magnitude so that the requirement $z_i \ll 1$ meant that the inequality Eq.(6.46) was automatically satisfied. However, we know that we must integrate over *all* transverse momenta of the gluons so that we sample 'corners' of transverse momentum space for which the inequality is violated. As we shall show below, these 'corners' can give rise to super-leading logarithms. These super-leading logarithms cancel when we consider inclusive processes for which we may apply dispersion techniques discussed in Chapter 3, but for

https://doi.org/10.1017/9781009290111.008 Published online by Cambridge University Press

certain exclusive processes they do *not* cancel and furnish the leading behaviour as $s \to \infty$.

Before imposing the constraints of angular ordering, it is necessary first to re-write the $t = 0$ BFKL equation in a form which will be suitable for the study of the more exclusive quantities. We can rewrite the $t = 0$ BFKL equation of Eq.(4.13) in the form

$$f_\omega(\mathbf{k}) = f_\omega^{(0)}(\mathbf{k}) + \bar{\alpha}_s \int \frac{d^2\mathbf{q}}{\pi \mathbf{q}^2} \int_0^1 \frac{dz}{z} z^\omega \Delta_R(z,k) \Theta(q-\mu) f_\omega(\mathbf{q}+\mathbf{k}), \quad (6.47)$$

where $\mathbf{q} = \mathbf{k}' - \mathbf{k}$ is the transverse momentum of the emitted gluon and the gluon Regge factor is

$$\ln \Delta_R(z,k) = -\bar{\alpha}_s \int_z^1 \frac{dz'}{z'} \int \frac{d^2\mathbf{q}}{\pi \mathbf{q}^2} \Theta(q-\mu)\Theta(k-q). \quad (6.48)$$

Equation (6.47) is easy to derive from Eq.(4.13) once we notice that

$$\ln \Delta_R(z,k) = 2 \ln(1/z)\, \epsilon_G(-k^2) \quad (6.49)$$

where $1+\epsilon_G(-k^2)$ is the gluon Regge trajectory derived in Chapter 3. In addition we used the fact that

$$\frac{1}{\omega - 2\epsilon_G(-k^2)} = \int_0^1 \frac{dz}{z} z^\omega \Delta_R(z,k). \quad (6.50)$$

The driving term, $f_\omega^{(0)}(\mathbf{k})$, includes the virtual corrections which reggeize the bare gluon. This form of the BFKL equation has a kernel which, under iteration, generates real gluon emissions with all the virtual corrections summed to all orders. As such, it is suitable for the study of the final state. Of course f_ω includes the sum over all final states and as such the μ-dependence cancels between the real and virtual contributions. However, we intend to investigate more exclusive quantities which are no longer infrared finite. The scale μ should then be regarded as the scale above which we can resolve real gluon emission.

Let us now take a specific example. We will look at the contributions to the structure function of an on-shell gluon which come from the emission of either one or two gluons which are constrained to have their transverse momentum less than some scale Q. The energy of the bare on-shell gluon is fixed, thus our

https://doi.org/10.1017/9781009290111.008 Published online by Cambridge University Press

boundary condition is

$$\begin{aligned} F^{(0)}(x,\mathbf{k}) &= \delta(x-1)\,\delta^2(\mathbf{k}), \qquad \text{i.e.} \\ f_\omega^{(0)}(\mathbf{k}) &= \delta^2(\mathbf{k}). \end{aligned} \tag{6.51}$$

Since the gluon is on shell it does not pick up any corrections due to the reggeization (i.e. we used $\epsilon_G(0) = 0$).

The structure function (defined by integrating over all $\mathbf{q_i}^2 \leq Q^2$) thus satisfies the equation,

$$\begin{aligned} F_\omega(Q^2,\mu^2) &= \Theta(Q-\mu) + \sum_{j=1}^{\infty}\prod_{i=1}^{j}\left\{\bar{\alpha}_s\int\frac{dz_i}{z_i}\frac{d^2\mathbf{q_i}}{\pi\mathbf{q_i}^2}\right. \\ &\times \left.\Delta_R(z_i,k_i)z_i^\omega\,\Theta(q_i-\mu)\Theta(Q-q_i)\right\}. \end{aligned} \tag{6.52}$$

and we have isolated the contributions from i real gluon emissions by iterating the kernel explicitly. Again non-boldface means the modulus of the two-vector.

Ignoring the coherence effects for the moment, the contribution to the structure function from the emission of a single gluon is thus

$$F_\omega^{(1)}(Q^2,\mu^2) = \bar{\alpha}_s\int_{\mu^2}^{Q^2}\frac{d^2\mathbf{q_1}}{\mathbf{q_1}^2}\int_0^1\frac{dz_1}{z_1}z_1^\omega\Delta_R(z_1,k_1) \tag{6.53}$$

and $\mathbf{k_1} = -\mathbf{q_1}$ (since the initial gluon is on shell). The Regge factor can then be integrated and yields,

$$\ln\Delta_R(z_1,q_1) = -\bar{\alpha}_s\ln(1/z_1)\ln q_1^2/\mu^2. \tag{6.54}$$

Let us compute our result as a power series in α_s, i.e. we expand the Regge exponential. Thus

$$\begin{aligned} F_\omega^{(1)}(Q^2,\mu^2) &= \bar{\alpha}_s\int_{\mu^2}^{Q^2}\frac{dq_1^2}{q_1^2}\int_0^1\frac{dz_1}{z_1}z_1^\omega \\ &\times\left[1-\bar{\alpha}_s\ln\frac{1}{z_1}\ln\frac{q_1^2}{\mu^2}+\frac{1}{2}\left(\bar{\alpha}_s\ln\frac{1}{z_1}\ln\frac{q_1^2}{\mu^2}\right)^2+\mathcal{O}(\alpha_s^3)\right]. \end{aligned} \tag{6.55}$$

The z_1-integral can be done by parts and yields

$$F_\omega^{(1)}(Q^2,\mu^2) = \frac{\bar{\alpha}_s}{\omega}\ln\frac{Q^2}{\mu^2}-\frac{1}{2}\left(\frac{\bar{\alpha}_s}{\omega}\ln\frac{Q^2}{\mu^2}\right)^2+\frac{1}{3}\left(\frac{\bar{\alpha}_s}{\omega}\ln\frac{Q^2}{\mu^2}\right)^3+\mathcal{O}(\alpha_s^4). \tag{6.56}$$

https://doi.org/10.1017/9781009290111.008 Published online by Cambridge University Press

Similarly, the contribution from two-gluon emission is

$$F_\omega^{(2)}(Q^2,\mu^2) = \bar{\alpha}_s^2 \int_{\mu^2}^{Q^2} \frac{d^2\mathbf{q_1}}{\pi \mathbf{q_1}^2} \frac{d^2\mathbf{q_2}}{\pi \mathbf{q_2}^2} \int_0^1 \frac{dz_1}{z_1} z_1^\omega \frac{dz_2}{z_2} z_2^\omega [1 + \mathcal{O}(\alpha_s)]$$
$$= \left(\frac{\bar{\alpha}_s}{\omega} \ln \frac{Q^2}{\mu^2} \right)^2 + \mathcal{O}(\alpha_s^3). \quad (6.57)$$

In fact, a more detailed treatment (Marchesini (1995)) reveals that the inclusive structure function satisfies

$$F_\omega(Q^2) \equiv \sum_{i=0}^{\infty} F_\omega^{(i)}(Q) = \left(\frac{Q^2}{\mu^2} \right)^{\bar{\gamma}}, \quad (6.58)$$

where $\bar{\gamma}$ is the BFKL anomalous dimension.

As we alluded to at the start of this section – these results (with the exception of Eq.(6.58)) are wrong. We must modify Eqs.(6.47) and (6.48) to account for coherence, so that Eq.(6.52) becomes

$$F_\omega(Q^2,\mu^2) = \Theta(Q-\mu) + \sum_{j=1}^{\infty} \prod_{i=1}^{j} \left\{ \bar{\alpha}_s \int \frac{dz_i}{z_i} \frac{d^2\mathbf{q_i}}{\pi \mathbf{q_i}^2} \right.$$
$$\left. \times \Delta(z_i,k_i) z_i^\omega \, \Theta(q_{i+1} - z_i q_i) \Theta(Q - q_i) \right\}, \quad (6.59)$$

where the coherence improved Regge factor is

$$\ln \Delta(z_i,k_i,q_i) = -\int_{z_i}^1 \frac{dz}{z} \int \frac{d^2\mathbf{q}}{\pi \mathbf{q}^2} \bar{\alpha}_s \Theta(q - z_i q_i) \Theta(k_i - q). \quad (6.60)$$

Let us now re-compute the single gluon emission cross-section. The Regge factor now becomes (because $k_1 = q_1$)

$$\ln \Delta(z_1,k_1,q_1) = -\bar{\alpha}_s \ln^2(1/z). \quad (6.61)$$

Expanding as a power series in α_s we now obtain

$$F_\omega^{(1)}(Q^2,\mu^2) = \bar{\alpha}_s \int_{\mu^2}^{Q^2} \frac{dq_1^2}{q_1^2} \int_0^{Q/k} \frac{dz_1}{z_1} z_1^\omega \left[1 - \bar{\alpha}_s \ln^2 \frac{1}{z} + \mathcal{O}(\alpha_s^2) \right]. \quad (6.62)$$

The z-integrals can again be performed using

$$\int_0^{Q/k} \frac{dz}{z} z^\omega = \frac{1}{\omega} + \mathcal{O}(1),$$
$$\int_0^{Q/k} \frac{dz}{z} z^\omega \ln^2 z = \frac{2}{\omega^3} + \mathcal{O}(1), \quad (6.63)$$

https://doi.org/10.1017/9781009290111.008 Published online by Cambridge University Press

and we neglect those terms which are not singular in the limit $\omega \to 0$ (which corresponds to keeping those terms which are leading in the Regge limit and beyond). Our final answer for the coherence improved calculation of the single gluon emission rate is therefore

$$F_\omega^{(1)}(Q^2,\mu^2) = \left[\frac{\bar{\alpha}_s}{\omega}\ln\frac{Q^2}{\mu^2} - 2\frac{\bar{\alpha}_s^2}{\omega^3}\ln\frac{Q^2}{\mu^2} + \cdots\right]. \tag{6.64}$$

Inverting the Mellin transform, we therefore see that the cross-section for single gluon emission is enhanced over the naive BFKL expectation by a factor of $\ln s$. This logarithm (and those that occur at higher orders in α_s) must be cancelled in the inclusive sum. We can therefore write the cross-section for two-gluon emission, i.e.

$$F_\omega^{(2)}(Q^2,\mu^2) = \left[\frac{1}{2}\left(\frac{\bar{\alpha}_s}{\omega}\ln\frac{Q^2}{\mu^2}\right)^2 + 2\frac{\bar{\alpha}_s^2}{\omega^3}\ln\frac{Q^2}{\mu^2} + \cdots\right]. \tag{6.65}$$

Although we expect coherence to affect the details of the final state dramatically, it also generates sub-leading corrections to the inclusive BFKL cross-section. These corrections are embodied in the solution to Eq.(6.59) and have been studied in the work of Kwiecinski, Martin & Sutton (1995).

Before finishing this chapter, a few words are in order regarding other processes that allow a study of the BFKL (hard) Pomeron in the $t = 0$ limit. In Section 6.3 we considered the associated jet production in deep inelastic scattering. By now, it should be clear that a similar process can be studied in hadron collider experiments (or in γ–p collisions with nearly on-shell photons), namely, events containing two jets which are produced so that they are separated by a large interval in rapidity (i.e. **double associated jet production**) (Mueller & Navalet (1987), Del Duca & Schmidt (1994a,b), Stirling (1994)). The hadron impact factors of Eq.(6.16) and Eq.(6.17) are then applied to each hadron-jet vertex. Similarly, rather than insisting on the production of a forward jet (or forward and backward jet pair) we could look for heavy quark production in these rapidity regions. The quark mass then provides the large scale in the impact factor(s) (see e.g. Catani, Ciafaloni & Hautmann (1990, 1991), Collins & Ellis (1991) and Levin, Ryskin, Shabelskii & Shuvaev (1991)).

https://doi.org/10.1017/9781009290111.008 Published online by Cambridge University Press

6.6 Summary

• The high energy limit of deep inelastic scattering corresponds to the limit of low Bjorken-x. The leading log $1/x$ approximation leads to the low-x behaviour which is characterized by the leading eigenvalue of the BFKL kernel, i.e. $F_2(x,Q^2) \sim x^{-\omega_0}(Q^2)^{1/2}$.

• The diffusion properties of the BFKL equation mean that a large contribution to the total deep inelastic cross-section can arise from the non-perturbative domain where the typical transverse momenta are not large.

• A process which is better suited to the application of perturbative QCD is that of associated jet production. The observation of an additional jet, travelling close to the direction defined by the incoming hadron, ensures the clean factorization of the non-perturbative dynamics into known parton distribution functions.

• The more conventional DGLAP formalism of deep inelastic scattering can be related to the BFKL approach. The leading twist contribution can be extracted from the BFKL calculation and can be shown to be equivalent to the soft gluon limit of the DGLAP equations (i.e. the limit in which only the singular parts of the all-orders DGLAP splitting functions are kept).

• The multi-Regge kinematics (i.e. the strong ordering of the longitudinal momentum fractions) used to compute the elastic-scattering amplitudes (and hence total inclusive cross-sections) via the BFKL equation is inappropriate for the consideration of more exclusive quantities. Coherence effects lead to additional logarithms in energy which only cancel in the inclusive sum.

6.7 Appendix A

In this appendix we compute the virtual photon impact factor required to compute the deep inelastic structure functions. In Fig. 6.7 we show two of the four diagrams which are needed (the other two are trivially obtained by reversing the direction of the quark line). Our calculation is very much analogous to that of Section 4.4.

https://doi.org/10.1017/9781009290111.008 Published online by Cambridge University Press

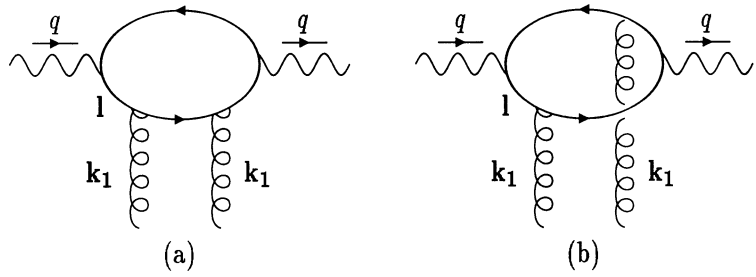

Fig. 6.7. Two of the four graphs used to compute the photon impact factor.

For Fig. 6.7(b), we have the amplitude

$$A^{\mu\nu\alpha\beta}_{(b)} = -(4\pi)^2\alpha_s\alpha\, e_q^2 \frac{\mathrm{Tr}(\hat{l}\gamma^\mu(\hat{l}-\hat{k_1})\gamma^\beta(\hat{l}-\hat{k_1}-\hat{q})\gamma^\nu(\hat{l}-\hat{q})\gamma^\alpha)}{l^2(l-k_1-q)^2}. \tag{A.6.1}$$

We use the notation $\hat{l}$ for $\gamma_\mu l^\mu$ and e_q is the quark charge in units of the proton charge. As in Section 4.4 we have factored out the colour factor. We express the four momenta l^μ, k_1^μ and q^μ in terms of the light-like vectors p_1^μ and p_2^μ ($p_2^\mu \equiv p^\mu$ is the incoming proton momentum) and their transverse components, i.e.

$$\begin{aligned} l^\mu &= \rho p_1^\mu + \lambda p_2^\mu + l_\perp^\mu \\ k_1^\mu &= \rho_1 p_1^\mu + \lambda_1 p_2^\mu + k_{1\perp}^\mu \\ q^\mu &= p_1^\mu - x p_2^\mu. \end{aligned}$$

The denominator factors are also as in Section 4.4, i.e.

$$\frac{1}{l^2}\frac{1}{(l-k_1-q)^2} = \frac{\rho(1-\rho)}{D_1 D_2}, \tag{A.6.2}$$

where

$$\begin{aligned} D_1 &= \mathbf{l}^2 + Q^2\rho(1-\rho) \\ D_2 &= (\mathbf{l}-\mathbf{k_1})^2 + Q^2\rho(1-\rho) \end{aligned}$$

(recall $Q^2 = -q^2 > 0$).

In the high energy limit we are only interested in those terms which are proportional to $p_1^\mu p_1^\nu$, i.e.

$$A^{\mu\nu\alpha\beta}_{(b)} = -(4\pi)^2\alpha\alpha_s e_q^2 \frac{\rho(1-\rho)}{D_1 D_2}(A^{\alpha\beta}_{(b)} p_1^\mu p_1^\nu + \ldots.) \tag{A.6.3}$$

https://doi.org/10.1017/9781009290111.008 Published online by Cambridge University Press

and the tensor associated with the $p_1^\mu p_1^\nu$ factor is given by

$$A_{(b)}^{\alpha\beta} = \frac{4}{W^4}\mathrm{Tr}[\hat{l}\hat{p}_2(\hat{l}-\hat{k}_1)\gamma^\beta(\hat{l}-\hat{k}_1-\hat{q})\hat{p}_2(\hat{l}-\hat{q})\gamma^\alpha]. \qquad \text{(A.6.4)}$$

We have used the fact that $2q\cdot p \approx W^2$ in the high energy limit.

Also, we need to contract with the photon polarization vectors. For longitudinal photons we contract with

$$\epsilon_\alpha^L \epsilon_\beta^{L*} = \frac{4Q^2}{W^2}\frac{p_{2\alpha}p_{2\beta}}{W^2} + \cdots, \qquad \text{(A.6.5)}$$

whilst for transverse photons we need to contract with

$$\sum \epsilon_\alpha^T \epsilon_\beta^{T*} = -g_{\alpha\beta} + \frac{4Q^2}{W^2}\frac{p_{2\alpha}p_{2\beta}}{W^2} + \cdots. \qquad \text{(A.6.6)}$$

The dots refer to terms which ultimately vanish since they contain factors $\sim q_\alpha q_\beta$ and $\sim q_\alpha p_{2\beta} + q_\beta p_{2\alpha}$. Such terms vanish since current conservation implies that their contraction with the leptonic tensor must vanish. Thus, on contracting the relevant components of the trace it follows (without too much work) that

$$\begin{aligned} -g_{\alpha\beta}A_{(b)}^{\alpha\beta} &= 16[\mathbf{l}\cdot(\mathbf{l}-\mathbf{k_1}) + \mathbf{k_1}^2\rho(1-\rho)] \qquad \text{(A.6.7)} \\ &= 8[D_1 + D_2 - 2Q^2\rho(1-\rho) - \mathbf{k_1}^2(\rho^2 + (1-\rho)^2)] \end{aligned}$$

and

$$\frac{4Q^2}{W^2}\frac{p_{2\alpha}p_{2\beta}}{W^2}A_{(b)}^{\alpha\beta} = 32Q^2\rho^2(1-\rho)^2. \qquad \text{(A.6.8)}$$

Thus, in the same notation as in Eqs.(4.38) and (4.39), we have the following contribution to the amplitudes from Fig. 6.7(b):

$$\begin{aligned} A_{(b)\Sigma}^{\mu\nu} &= -(4\pi)^2\alpha_s\alpha\, e_q^2\frac{8\rho(1-\rho)}{D_1D_2}p_1^\mu p_1^\nu \\ &\times \left\{D_1 + D_2 - 2Q^2\rho(1-\rho) - \mathbf{k_1}^2[\rho^2 + (1-\rho)^2]\right\} \qquad \text{(A.6.9)} \end{aligned}$$

and

$$A_{(b)L}^{\mu\nu} = -(4\pi)^2\alpha_s\alpha\, e_q^2\frac{32\rho(1-\rho)}{D_1D_2}p_1^\mu p_1^\nu\left\{Q^2\rho^2(1-\rho)^2\right\}. \qquad \text{(A.6.10)}$$

and $A_{(b)\Sigma}^{\mu\nu}$ is defined such that the amplitude for scattering transverse photons is

$$(A_{(b)\Sigma}^{\mu\nu} + A_{(b)L}^{\mu\nu})/2.$$

https://doi.org/10.1017/9781009290111.008 Published online by Cambridge University Press

We can now follow the steps of Section 4.4 to deduce the corresponding contributions to the impact factors:

$$\Phi^{\Sigma}_{(b)}(\mathbf{k_1}) = -8\alpha\alpha_s \sum_{q=1}^{n_f} e_q^2 \int d\rho\, d^2\mathbf{l} \times \left\{ \frac{1}{D_1} + \frac{1}{D_2} - \frac{2Q^2\rho(1-\rho) + \mathbf{k_1^2}[\rho^2 + (1-\rho)^2]}{D_1 D_2} \right\} \quad \text{(A.6.11)}$$

and

$$\Phi^{L}_{(b)}(\mathbf{k_1}) = -32\alpha\alpha_s \sum_{q=1}^{n_f} e_q^2 \int d\rho\, d^2\mathbf{l} \left\{ Q^2 \frac{\rho^2(1-\rho)^2}{D_1 D_2} \right\}. \quad \text{(A.6.12)}$$

A factor of 2 has been included to account for the related graph which has the quark line circulating in the opposite direction, and we have summed over all n_f flavours of quark.

Fortunately, we do not need to do any more work in order to extract the contribution from the graph shown in Fig. 6.7(a). It is related to the above impact factor via

$$\Phi^{\lambda}_{(a)}(\mathbf{k}) = -\Phi^{\lambda}_{(b)}(\mathbf{0}). \quad \text{(A.6.13)}$$

Using this, and noting that

$$\int d^2\mathbf{l} \frac{1}{D_1^n} = \int d^2\mathbf{l} \frac{1}{D_2^n}, \quad \text{(A.6.14)}$$

we can write the complete impact factors for deep inelastic scattering as

$$\Phi_{\Sigma}(\mathbf{k_1}) = 8\alpha\alpha_s \sum_{q=1}^{n_f} e_q^2 \int d\rho\, d^2\mathbf{l} \times \left\{ \frac{\mathbf{k_1^2}[\rho^2 + (1-\rho)^2]}{D_1 D_2} - Q^2\rho(1-\rho)\left(\frac{1}{D_1} - \frac{1}{D_2}\right)^2 \right\} \quad \text{(A.6.15)}$$

and

$$\Phi_L(\mathbf{k_1}) = 16\alpha\alpha_s \sum_{q=1}^{n_f} e_q^2 \int d\rho\, d^2\mathbf{l} \left\{ Q^2\rho^2(1-\rho)^2 \left(\frac{1}{D_1} - \frac{1}{D_2}\right)^2 \right\}. \quad \text{(A.6.16)}$$

The transverse polarization impact factor, Φ_T, is given by

$$\Phi_T = \frac{1}{2}(\Phi_{\Sigma} + \Phi_L). \quad \text{(A.6.17)}$$

https://doi.org/10.1017/9781009290111.008 Published online by Cambridge University Press

Using Eq.(6.2), we can now deduce the impact factor for the sum of transverse and longitudinal cross-sections:

$$\Phi_2(\mathbf{k_1}) = \Phi_T(\mathbf{k_1}) + \Phi_L(\mathbf{k_1}) = \frac{\Phi_\Sigma(\mathbf{k_1}) + 3\Phi_L(\mathbf{k_1})}{2}. \quad \text{(A.6.18)}$$

As in Section 4.4, we can go further and perform the $\mathbf{l}$ integral at the expense of introducing a Feynman parameter, τ. We need to use

$$\int \frac{d^2\mathbf{l}}{D_1^2} = \int \frac{d^2\mathbf{l}}{D_2^2} = \frac{\pi}{\rho(1-\rho)Q^2} \quad \text{(A.6.19)}$$

and

$$\int \frac{d^2\mathbf{l}}{D_1 D_2} = \int_0^1 d\tau \frac{\pi}{\rho(1-\rho)Q^2 + \tau(1-\tau)\mathbf{k_1}^2}. \quad \text{(A.6.20)}$$

After some simple algebra, we then obtain

$$\begin{aligned}\Phi_T(\mathbf{k_1}) &= 4\pi\alpha\alpha_s \sum_{q=1}^{n_f} e_q^2 \int_0^1 d\rho d\tau \frac{\mathbf{k_1}^2}{\rho(1-\rho)Q^2 + \tau(1-\tau)\mathbf{k_1}^2} \\ &\quad \times [\tau^2 + (1-\tau)^2][\rho^2 + (1-\rho)^2] \quad \text{(A.6.21)}\end{aligned}$$

and

$$\begin{aligned}\Phi_L(\mathbf{k_1}) &= 32\pi\alpha\alpha_s \sum_{q=1}^{n_f} e_q^2 \int_0^1 d\rho d\tau \frac{\mathbf{k_1}^2}{\rho(1-\rho)Q^2 + \tau(1-\tau)\mathbf{k_1}^2} \\ &\quad \times [\rho(1-\rho)\tau(1-\tau)]. \quad \text{(A.6.22)}\end{aligned}$$

6.8 Appendix B

The saddle point method of integration is a powerful tool for approximating integrals which may be cast into the form

$$\int_{-\infty}^{\infty} dx\, g(x) e^{-f(x)}. \quad \text{(B.6.1)}$$

The method is valid provided the function $f(x)$ has a minimum at some value $x = x_0$ and that it is 'very convex' in that region. This means that the nth derivative, $f^{(n)}(x)$, of $f(x)$ obeys the inequality

$$f^{(n)}(x_0) \ll \left(f^{(2)}(x_0)\right)^{n/2},$$

so that $f(x)$ may be approximated by

$$f(x) \approx f(x_0) + \frac{1}{2} f^{(2)}(x_0)\,(x - x_0)^2 \quad \text{(B.6.2)}$$

https://doi.org/10.1017/9781009290111.008 Published online by Cambridge University Press

(the first derivative vanishes at $x = x_0$ since $f(x)$ has a minimum there).

Furthermore, the function $g(x)$ is assumed to be a 'slowly varying' function at $x = x_0$. This means that it may be approximated by its value at $x = x_0$ or, in cases where that value vanishes, by its first non-vanishing even order derivative at $x = x_0$, i.e. if the first non-vanishing even order derivative at $x = x_0$ is the $(2m)$th derivative then we write

$$g(x) \approx \frac{1}{(2m)!} g^{(2m)}(x_0)\,(x - x_0)^{2m}. \tag{B.6.3}$$

Substituting Eqs.(B.6.2) and (B.6.3) into Eq.(B.6.1) and changing variables to $y = (x - x_0)$ we obtain the Gaussian integral

$$e^{-f(x_0)} \int_{-\infty}^{\infty} dy\, \frac{1}{(2m)!} g^{(2m)}(x_0) y^{2m} \exp\left(-\frac{1}{2} f^{(2)}(x_0) y^2\right)$$
$$= \frac{\sqrt{2\pi}}{2^m m!} \frac{g^{(2m)}(x_0)}{(f^{(2)}(x_0))^{m+1/2}} e^{-f(x_0)}. \tag{B.6.4}$$

The corrections to the above approximation are of order

$$\frac{f^{(n)}(x_0)}{(f^{(2)}(x_0))^{n/2}} \quad \text{or} \quad \frac{g^{(2m+2)}(x_0)}{g^{(2m)}(x_0) f^{(2)}(x_0)}.$$

https://doi.org/10.1017/9781009290111.008 Published online by Cambridge University Press